

Electronic Supplementary Information

Influence of CH₂Cl₂ for the structure stabilization of the Ni^{II} complex [Ni{6-MeO(O)CC₆H₄NHC(S)NP(S)(O*i*Pr)₂-1,5-S,S'}₂]·CH₂Cl₂

Maria G. Babashkina,^a Damir A. Safin,*^a Monika Srebro,^b Piotr Kubisiak,^b Mariusz Mitoraj,^{b*} Michael Bolte^c and Yann Garcia^a

^a Institute of Condensed Matter and Nanosciences, MOST - Inorganic Chemistry, Université Catholique de Louvain, Place L. Pasteur 1, 1348 Louvain-la-Neuve, Belgium. Fax: +32(0) 1047 2330; Tel: +32(0) 1047 2831; E-mail: damir.safin@ksu.ru

^b Department of Theoretical Chemistry, Faculty of Chemistry, Jagiellonian University, R. Ingardena 3, 30-060 Cracow, Poland. Email: mitoraj@chemia.uj.edu.pl.

^c Institut für Anorganische Chemie J.-W.-Goethe-Universität, Frankfurt/Main, Germany.

Physical measurements: Infrared spectra (Nujol) were recorded with a Thermo Nicolet 380 FT-IR spectrometer in the range 400–3600 cm⁻¹. NMR spectra were obtained on a Bruker Avance 300 MHz spectrometer at 25 °C. ¹H and ³¹P{¹H} NMR spectra were recorded at 299.948 and 121.420 MHz, respectively. Chemical shifts are reported with reference to SiMe₄ (¹H) and 85% H₃PO₄ (³¹P{¹H}). Electronic spectra of absorption in 10⁻⁴ M solution were measured on a Lambda-35 spectrometer in the range 200–1000 nm. Cyclic voltammetry was carried out at 100 mV/s scan rate in 0.1 M *n*Bu₄NPF₆ solutions using a three-electrode configuration (glassy carbon electrode, Pt counter electrode, Ag/AgCl reference) and a Gamry Series G 750 potentiostat and function generator. The ferrocene/ferrocenium couple served as internal standard. Elemental analyses were performed on a Thermoquest Flash EA 1112 Analyzer from CE Instruments.

Synthesis of [NiL₂]: A suspension of **HL** (3 mmol, 1.17 g) in aqueous EtOH (10 mL) was mixed with an aqueous EtOH (10 mL) solution of KOH (3.3 mmol, 0.18 g). An aqueous (10 mL) solution of NiCl₂ (1.9 mmol, 0.25 g) was added dropwise under vigorous stirring to the resulting potassium salt. The mixture was stirred at room temperature for a further 3 h and left overnight. The resulting complex was extracted with CH₂Cl₂, washed with water and dried with anhydrous MgSO₄. The solvent was then removed in vacuo. Dark violet crystals were isolated by recrystallisation from a 1:3 mixture of CH₂Cl₂ and *n*-hexane. Yield 0.276 g (79%). IR ν (cm⁻¹): 566 (P=S), 977 (POC), 1528 (SCN), 1690 (C=O), 3195 (NH). ¹H NMR δ (ppm): 1.44 (d, ³J_{H,H} = 6.1 Hz, 12H, CH₃, *i*Pr), 1.54 (d, ³J_{H,H} = 6.1 Hz, 12H, CH₃, *i*Pr), 3.92 (s, 6H, CH₃, Me), 5.09 (d. sept, ³J_{POCH} = 10.1 Hz, ³J_{H,H} = 6.2 Hz, 4H, OCH), 6.99 (br. t, ³J_{H,H} = 8.4 Hz, 2H, *p*-H, C₆H₄), 7.41 (d. t, ³J_{H,H} = 7.9 Hz, ⁴J_{H,H} = 1.6 Hz, 2H, *m*-H, C₆H₄), 7.97 (d. d, ³J_{H,H} = 8.0 Hz, ⁴J_{H,H} = 1.6 Hz, 2H, *o*-H, C₆H₄), 8.57 (d, ³J_{H,H} = 8.5 Hz, 2H, *m*-H, C₆H₄), 11.21 (d, ⁴J_{PNCNH} = 6.6 Hz, 2H, arylNH); ³¹P{¹H} NMR δ (ppm): 51.1; Anal. Calc. for C₃₀H₄₄N₄NiO₈P₂S₄ (837.58): C 43.02, H 5.29, N 6.69. Found: C 42.93, H 5.20, N 6.64%.

DFT calculations: We have applied in DFT-based geometry optimizations the hybrid exchange-correlation functional B3LYP¹ and the LANL2DZ basis set by Wadt and Hay,² as implemented in the Gaussian 09 package.³ Deformation density map as well as deformation density contributions of the ETS-NOCV method were plotted based on ADF-GUI interface.⁴

ETS-NOCV bonding analysis: Historically the Natural Orbitals for Chemical Valence (NOCV) have been derived from the Nalewajski-Mrozek valence theory as eigenvectors that diagonalizes the deformation density matrix. It was shown that the natural orbitals for chemical valence pairs (ψ_{-k}, ψ_k) decompose the differential density $\Delta\rho$ into NOCV-contributions ($\Delta\rho_k$):

$$\Delta\rho(r) = \sum_{k=1}^{M/2} v_k [-\psi_{-k}^2(r) + \psi_k^2(r)] = \sum_{k=1}^{M/2} \Delta\rho_k(r) \quad (1)$$

where v_k and M stand for the NOCV eigenvalues and the number of basis functions, respectively. Visual inspection of deformation density plots ($\Delta\rho_k$) helps to attribute symmetry and the direction of the charge flow. In addition, these pictures are enriched by providing the energetic estimations, $\Delta E_{orb}(k)$, for each $\Delta\rho_k$ within ETS-NOCV scheme. The exact formula which links ETS and NOCV method will be given in the next paragraph, after we briefly present the basic concept of ETS scheme. In this method the total bonding energy ΔE_{total} between interacting fragments exhibiting the geometry as in the combined complex is divided into the three components:

$$\Delta E_{total} = \Delta E_{elstat} + \Delta E_{Pauli} + \Delta E_{orb} \quad (2)$$

The first term, ΔE_{elstat} , corresponds to the classical electrostatic interaction between the promoted fragments as they are brought to their positions in the final complex. The second term, ΔE_{Pauli} , accounts for the repulsive Pauli interaction between occupied orbitals on the two fragments in the combined molecule. Finally, the last stabilizing term, ΔE_{orb} represents the interactions between the occupied molecular orbitals of one fragment with the unoccupied molecular orbitals of the other fragment as well as mixing of occupied and virtual orbitals within the same fragment (inner-fragment polarization). This energy term may be linked to the electronic bonding effect coming from the formation of a chemical bond. The three last terms (ΔE_{elstat} , ΔE_{Pauli} , ΔE_{orb}) very often are combined into the instantaneous interaction energy, ΔE_{int} , as it describes the interaction between the fragments in the geometry of the complex.

In the combined ETS-NOCV scheme the orbital interaction term (ΔE_{orb}) is expressed in terms of NOCV's eigenvalues (v_k) as:

$$\Delta E_{orb} = \sum_k \Delta E_{orb}(k) = \sum_{k=1}^{M/2} v_k [-F_{-k,-k}^{TS} + F_{k,k}^{TS}] \quad (3)$$

where $F_{i,i}^{TS}$ are diagonal Kohn-Sham matrix elements defined over NOCV with respect to the transition state (TS) density (at the midpoint between density of the molecule and the sum of fragment densities). The above

components $\Delta E_{\text{orb}}(k)$ provide the energetic estimation of $\Delta\rho_k$ that may be related to the importance of a particular electron flow channel for the bonding between the considered molecular fragments. ETS-NOCV analysis was done based on the Amsterdam Density Functional (ADF) package in which this scheme was implemented.

From the results of DFT calculations we concluded that the *trans*-1,3-*N,S* isomer is more stable (by 3.6 kcal/mol) than the corresponding *trans*-1,5-*S,S'* conformation (see Fig. S1). In order to shed some light on the origin of such trend we described the bonding between amine-containing fragment and the rest of the complex (black circle line in Fig. S2 indicates the fragmentation pattern). The bonding analysis was performed using the ETS-NOCV scheme as implemented in the Amserdam Density Functional (ADF) package, version 2009.01.⁴ The main contribution, exhibiting the formation of $\sigma(\text{HN}-\text{C})$ bonding, originates from the charge transfer $\Delta\rho_1$ (Fig. S2), with the highest stabilization observed for the **[Ni(L-1,3-*N,S*)₂]** isomer. The π -component of the N–C bond in both isomers, $\Delta\rho_2$, is quantitatively far less important (see $\Delta E_{\text{orb}}(2)$ in Table S3) and also dominates for the **[Ni(L-1,3-*N,S*)₂]** conformation. Such a domination originates from the formation of intramolecular NH···S interaction in **[Ni(L-1,3-*N,S*)₂]**, see $\Delta\rho_2$. More pronounced charge transfers ($\Delta\rho_1$ and $\Delta\rho_2$) for **[Ni(L-1,3-*N,S*)₂]** are reflected by more stabilizing ΔE_{orb} values, what in turn determines the trend in total interaction energy values, ΔE_{total} , see Table S3. Thus, higher stabilization of the **[Ni(L-1,3-*N,S*)₂]** isomer vs. the **[Ni(L-1,5-*S,S'*)₂]** complex can be related to the stronger amine bonding as well as the presence of intramolecular NH···S interaction.

X-Ray crystallography: The X-ray data were collected on a STOE IPDS-II diffractometer with graphite-monochromatised Mo-K α radiation generated by a fine-focus X-ray tube operated at 50 kV and 40 mA. The reflections of the images were indexed, integrated and scaled using the X-Area data reduction package.⁵ Data were corrected for absorption using the PLATON program.⁶ The structures were solved by direct methods using the SHELXS-97 program⁷ and refined first isotropically and then anisotropically using SHELXL-97.⁷ Hydrogen atoms were revealed from $\Delta\rho$ maps and those bonded to C were refined using appropriate riding models. H atoms bonded to N were freely refined. Figures were generated using the program Mercury.⁸

Crystal data for [NiL₂]·CH₂Cl₂. C₃₁H₄₆Cl₂N₄NiO₈P₂S₄, $M_r = 922.51 \text{ g mol}^{-1}$, triclinic, space group $P\bar{1}$, $a = 9.3129(4)$, $b = 13.0620(5)$, $c = 18.7085(7)$ Å, $\alpha = 79.439(2)$, $\beta = 84.354(2)$, $\gamma = 69.584(2)^\circ$, $V = 2095.25(14)$ Å³, $Z = 2$, $\rho = 1.462 \text{ g cm}^{-3}$, $\mu(\text{Mo-K}\alpha) = 0.916 \text{ mm}^{-1}$, reflections: 56997 collected, 15238 unique, $R_{\text{int}} = 0.0252$, $R_1(\text{all}) = 0.0522$, $wR_2(\text{all}) = 0.0919$.

CCDC 805254 contains the supplementary crystallographic data. These data can be obtained free of charge via <http://www.ccdc.cam.ac.uk/conts/retrieving.html>, or from the Cambridge Crystallographic Data Centre, 12 Union Road, Cambridge CB2 1EZ, UK; fax: (+44) 1223-336-033; or e-mail: deposit@ccdc.cam.ac.uk.

References

- 1 (a) J. P. Perdew, *Phys. Rev. B: Condens. Matter.*, 1986, **33**, 8822; (b) A. D. Becke, *J. Chem. Phys.*, 1993, **98**, 1372.
- 2 M. J. Frisch, G.W. Trucks, H. B. Schlegel, G. E. Scuseria, M.A. Robb, J. R. Cheeseman, G. Scalmani, V. Barone, B. Mennucci, G. A. Petersson, H. Nakatsuji, M. Caricato, X. Li, H. P. Hratchian, A. F. Izmaylov, J. Bloino, G. Zheng, J. L. Sonnenberg, M. Hada, M. Ehara, K. Toyota, R. Fukuda, J. Hasegawa, M. Ishida, T. Nakajima, Y. Honda, O. Kitao, H. Nakai, T. Vreven, J. A. Montgomery Jr., J. E. Peralta, F. Ogliaro, M. Bearpark, J. J. Heyd, E. Brothers, K. N. Kudin, V. N. Staroverov, R. Kobayashi, J. Normand, K. Raghavachari, A. Rendell, J. C. Burant, S. S. Iyengar, J. Tomasi, M. Cossi, N. Rega, J. M. Millam, M. Klene, J. E. Knox, J. B. Cross, V. Bakken, C. Adamo, J. Jaramillo, R. Gomperts, R. E. Stratmann, O. Yazyev, A. J. Austin, R. Cammi, C. Pomelli, J. W. Ochterski, R. L. Martin, K. Morokuma, V.G. Zakrzewski, G. A. Voth, P. Salvador, J. J. Dannenberg, S. Dapprich, A. D. Daniels, O. Farkas, J. B. Foresman, J. V. Ortiz, J. Cioslowski, D. J. Fox, Gaussian 09, Gaussian Inc., Wallingford CT, 2009.
- 3 P. J. Hay, W. R. Wadt, *J. Chem. Phys.*, 1985, **82**, 270.
- 4 ADF-GUI 2009.01, SCM, Amsterdam, The Netherlands, <http://www.scm.com> (O. Visser, P. Leyronnas, W. J. van Zeist and M. Lupki).
- 5 Stoe & Cie. X-AREA. Area-Detector Control and Integration Software. Stoe & Cie, Darmstadt, Germany, 2001.
- 6 A. L. Spek, *Acta Crystallogr.*, 2009, **D65**, 148.
- 7 G. M. Sheldrick, *Acta Crystallogr.*, 2008, **A64**, 112.
- 8 I. J. Bruno, J. C. Cole, P. R. Edgington, M. Kessler, C. F. Macrae, P. McCabe, J. Pearson and R. Taylor, *Acta Crystallogr.*, 2002, **B58**, 389.

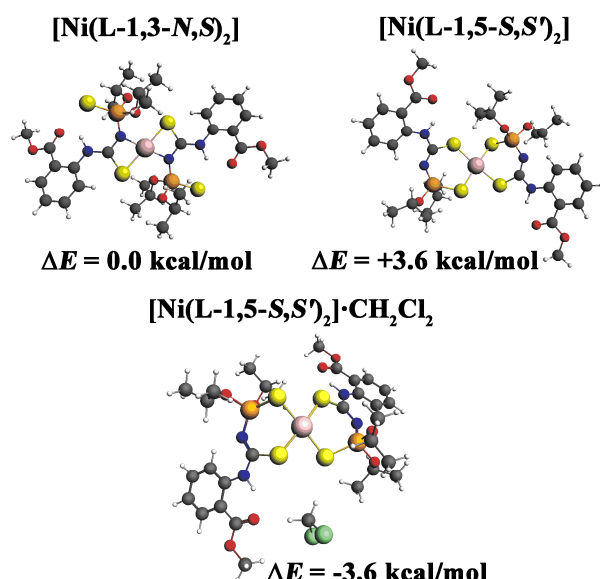


Fig. S1 Optimized structures of the isomers $[\text{Ni}(\text{L-1,3-}\text{N},\text{S})_2]$, $[\text{Ni}(\text{L-1,5-}\text{S},\text{S}')_2]$ and $[\text{Ni}(\text{L-1,5-}\text{S},\text{S}')_2]\text{-CH}_2\text{Cl}_2$ together with the relative energies obtained from DFT/B3LYP calculations.

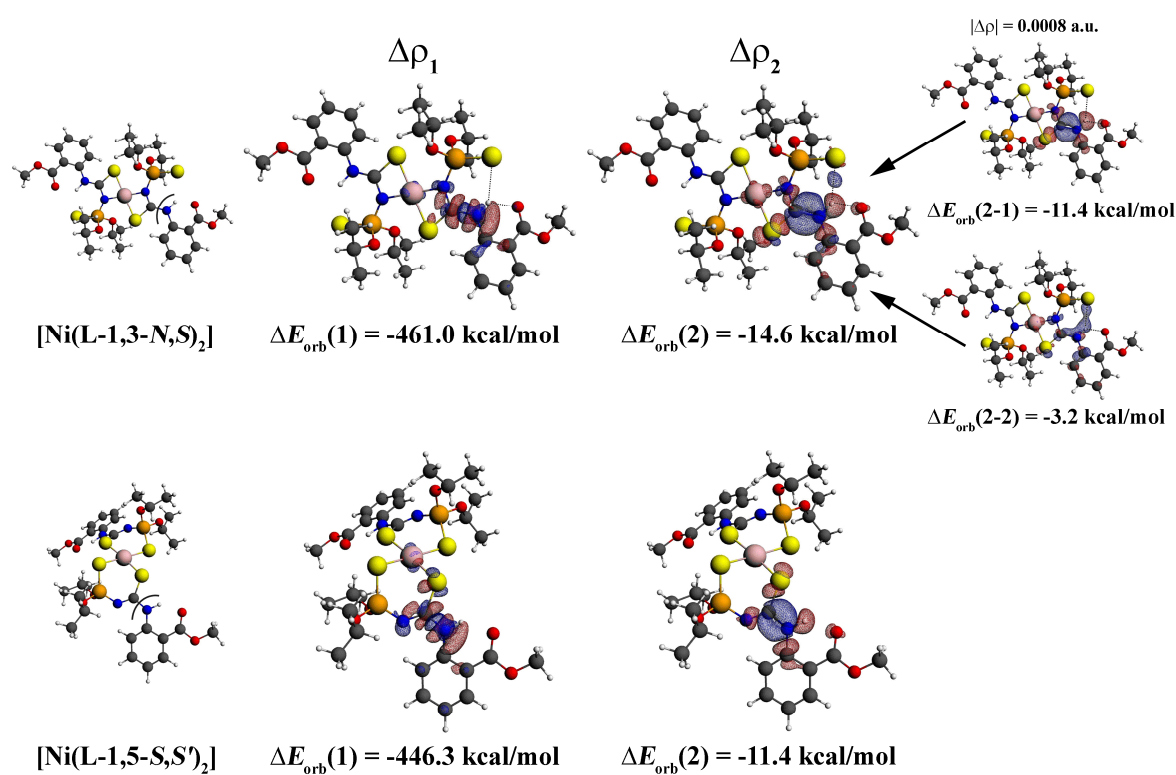


Fig. S2 The ETS-NOCV based results (deformation densities $\Delta\rho_i$ and corresponding energies ΔE_{orb} (i)) for the *trans*-isomers of $[\text{Ni}(\text{L-1,3-}\text{N},\text{S})_2]$ and $[\text{Ni}(\text{L-1,5-}\text{S},\text{S}')_2]$. Red color of $\Delta\rho_i$ shows charge depletion, whereas blue charge accumulation upon bond formation. The contour value of 0.005 a.u. was used for $\Delta\rho_1$, whereas 0.001 a.u. for $\Delta\rho_2$.

Table S1. Selected bond lengths (\AA) and angles ($^\circ$) for $[\text{NiL}_2]\cdot\text{CH}_2\text{Cl}_2$

<i>Bond lengths</i>					
Ni1–S1	2.2194(4)	N2–C1	1.3628(17)	P1–O2	1.5631(10)
Ni1–S1'	2.2036(4)	N2–C1'	1.3620(17)	P1–O2'	1.5664(10)
Ni1–S2	2.1982(4)	P1–N1	1.6094(12)	S1–P1	1.9934(6)
Ni1–S2'	2.1956(4)	P1–N1'	1.6084(12)	S1–P1'	1.9949(6)
N1–C1	1.3027(17)	P1–O1	1.5603(11)	S2–C1	1.7494(14)
N1–C1'	1.3072(17)	P1–O1'	1.5571(11)	S2–C1'	1.7504(14)
<i>Bond angles</i>					
Ni1–S1–P1	101.29(2)	O1–P1–O2	102.86(6)	S1–P1–N1	115.45(5)
Ni1–S1'–P1'	103.34(2)	O1'–P1'–O2'	104.34(6)	S1'–P1'–N1'	116.73(5)
Ni1–S2–C1	118.47(5)	P1–N1–C1	122.63(10)	S1–P1–O1	114.29(5)
Ni1–S2'–C1'	119.48(5)	P1'–N1'–C1'	122.80(10)	S1'–P1'–O1'	114.33(4)
N1–C1–N2	120.69(13)	S1–Ni1–S1'	177.57(2)	S1–P1–O2	109.05(5)
N1'–C1'–N2'	120.54(13)	S1–Ni1–S2	98.55(2)	S1'–P1'–O2'	107.20(4)
O1–P1–N1	106.43(6)	S1–Ni1–S2'	82.49(1)	S2–C1–N1	129.68(10)
O1'–P1'–N1'	105.68(6)	S1'–Ni1–S2	80.60(1)	S2'–C1'–N1'	130.03(10)
O2–P1–N1	107.86(6)	S1'–Ni1–S2'	98.46(2)	S2–C1–N2	109.61(10)
O2'–P1'–N1'	107.73(6)	S2–Ni1–S2'	177.34(2)	S2'–C1'–N2'	109.40(10)
<i>Torsion angles</i>					
Ni1–S2–C1–N1	16.35(16)	S2–Ni1–S1'–P1'	-142.59(2)	O1'–P1'–N1'–C1'	-81.04(13)
Ni1–S2'–C1'–N1'	-8.74(16)	S2'–Ni1–S1'–P1'	39.93(2)	O2–P1–N1–C1	-170.71(12)
Ni1–S2–C1–N2	-165.34(9)	N1–P1–S1–Ni1	67.80(5)	O2'–P1'–N1'–C1'	167.88(12)
Ni1–S2'–C1'–N2'	173.15(8)	N1'–P1'–S1'–Ni1	-63.83(5)	S1–P1–N1–C1	-48.49(13)
S1–Ni1–S2–C1	11.27(6)	O1–P1–S1–Ni1	-56.16(5)	S1'–P1'–N1'–C1'	47.30(13)
S1–Ni1–S2'–C1'	163.92(6)	O2–P1–S1–Ni1	-170.62(4)	P1–N1–C1–N2	-177.69(11)
S1'–Ni1–S2–C1	-171.04(6)	O1'–P1'–S1'–Ni1	60.21(5)	P1'–N1'–C1'–N2'	171.78(11)
S1'–Ni1–S2'–C1'	-13.82(6)	O2'–P1'–S1'–Ni1	175.33(4)	P1–N1–C1–S2	0.5(2)
S2–Ni1–S1–P1	-41.53(2)	O1–P1–N1–C1	79.49(13)	P1'–N1'–C1'–S2'	-6.2(2)
S2'–Ni1–S1–P1	136.01(2)				

Table S2. Hydrogen bond lengths (\AA) and angles ($^\circ$) for $[\text{NiL}_2]\cdot\text{CH}_2\text{Cl}_2$

D–H \cdots A	$d(\text{D–H})$	$d(\text{H}\cdots\text{A})$	$d(\text{D}\cdots\text{A})$	$\angle(\text{DHA})$
N2–H2 \cdots O3	0.81(2)	1.98(2)	2.6558(16)	141.8(19)
N2'–H2' \cdots O3'	0.83(2)	1.94(2)	2.6435(16)	142.6(19)
C1L–H1L1 \cdots O3	0.99	2.45	3.221(3)	134
C1L–H1L2 \cdots S2	0.99	2.95	3.90	161.2

Table S3. ETS-NOCV energy decomposition results (in kcal/mol), describing the interaction between the CH₃O(O)CC₆H₄NH group and Ni-based fragments in the *trans*-isomers of [Ni(L-1,3-N,S)₂] (upper line) and [Ni(L-1,5-S,S')₂] (bottom line).

ΔE_{orb}	ΔE_{Pauli}	ΔE_{elstat}	$\Delta E_{\text{total}}^a$	$\Delta E_{\text{orb}(1)}$	$\Delta E_{\text{orb}(2)}$
-488.8	677.5	-291.8	-103.1	-461.0	-14.6
-473.8	680.8	-301.6	-94.6	-446.3	-11.4

^a $\Delta E_{\text{total}} = \Delta E_{\text{orb}} + \Delta E_{\text{Pauli}} + \Delta E_{\text{elstat}}$